

**A pair of forward and reverse slow-mode shocks  
detected by Ulysses at ~ 5AU**

**C. M. Ho<sup>1</sup>, B. T. Tsurutani<sup>1</sup>, N. Lin<sup>2</sup>, L. J. Lanzerotti<sup>3</sup>, E.J. Smith<sup>1</sup>,  
B.E.Goldstein<sup>1</sup>, G. S. Lakhina<sup>1</sup>, and B. Buti<sup>1</sup>**

**<sup>1</sup>Jet Propulsion Laboratory, California Institute of Technology, Pasadena, CA 91109**

**<sup>2</sup>School of Physics and Astronomy, University of Minnesota, Minneapolis, MN 55455**

**<sup>3</sup>Bell Laboratories, Lucent Technologies, Murray Hill, NJ 07974**

**To be submitted to Geophysical Research Letters**

**First Version on February 10, 1998**

**Second Revision on May 1, 1998**

**Abstract:** We report the first finding of a pair of forward and reverse slow-mode shocks in the distant heliosphere using plasma and magnetic field data from the Ulysses spacecraft located at 5.3 AU and 9° S heliolatitude. The slow-mode shocks are found to occur in a compressed magnetic field region within a co-rotating interaction region (CIR). We find the slow shock Mach numbers to be 0.3-0.5, respectively. Across the shocks, the solar wind velocities jump by at least 40 km/s. The increases in plasma density and ion temperature accompany a decrease in the magnetic field  $B$ . The shocks are also found to have velocities of 60 km/s and 115 km/s and thicknesses between  $7.5 - 12.6 \times 10^4$  km (much larger than the ion inertial length,  $\sim 10^3$  km). Low frequency plasma waves are detected by the Ulysses URAP instrument at the slow-mode shock transition regions. However, the waves are not of sufficient amplitude to provide enough anomalous resistivity through wave-particle interactions for the shock dissipation. Low energy ( $\sim 30 - 90$  keV) electron enhancements directed along the local magnetic field are also found associated with the slow shocks, indicating the ability of the shocks to accelerate interplanetary particles.

## Introduction

Interplanetary slow-mode shocks are fundamental micro-structures of the solar wind, which are of interest from the points of view of space plasma theory and heliospheric dynamics. Slow-mode shocks may play an important role in interplanetary space in magnetic reconnection [Petschek, 1964] and, thus, the heating of the solar wind plasma [Pizzo, 1985]. Slow shocks can result from the steepening of MHD slow-mode waves. It is most probable that slow-mode shocks are generated in interplanetary regions [Barnes, 1966; Richter, 1991] where collisionless damping of slow-mode waves is small and the linear damping time exceeds the steepening time (i.e., plasma  $\beta < 1$  and  $T_i / T_e < 1$ ). However, even though in the last several decades a significant amount of solar wind data have been accumulated, only a limited number of interplanetary slow-mode shocks have been reported/identified [Chao and Olbert, 1970; Burlaga and Chao, 1971; Richter, 1987].

Magnetohydrodynamic (MHD) theory [Kennel et al., 1985] shows that both fast and slow-mode shocks can propagate either away from (forward shocks) or towards (reverse shocks) the sun with respect to the solar wind frame. At large heliospheric distances, when a corotating high speed solar wind overtakes a low speed solar wind, a pair of forward and reverse fast shocks are usually formed [Smith and Wolfe, 1976]. Similar to the fast mode shocks, a pair of forward and reverse slow-mode shocks are expected to exist. Within MHD there exists the possibility that slow shocks can be generated behind fast shocks with non-zero normal magnetic field components (the so-called Riemann problem) [Rosenau and Suess, 1977]. These slow-mode shocks should have opposite magnetic field structures, compared with the fast shocks. Across the shock, the plasma density, temperature and bulk velocity increase, and the magnetic field decreases as schematically illustrated in Figure 1. Thus there is a higher plasma beta ( $\beta$ ) region between the shocks than in the region outside them. We report here the discovery of a pair of forward and reverse slow-mode shocks through an extensive search of Ulysses interplanetary data.

## Data and Method

The magnetic field (1 s time resolution) and plasma (4 min maximum sample rate) data measured on Ulysses are used for the slow-mode shock search and identification. The coordinate system is a RTN system, where  $\vec{R}$  is the radial direction from the Sun,  $\vec{T} = \vec{\Omega} \times \vec{R} / |\vec{\Omega} \times \vec{R}|$  ( $\vec{\Omega}$  is the solar rotation axis), and  $\vec{N}$  completes the right-hand system.

Plasma wave data and energetic particle data measured on Ulysses are also used to identify their associated signatures with the slow shocks. All instrumentation descriptions can be found in the Supplementary Serials (Volume 92) of *Astronomy and Astrophysics* [1992].

The method used to identify the slow shocks is similar to that developed in a study of slow shocks in the geomagnetic tail [Ho et al., 1996]. We first determine if both conditions of  $\beta < 1$  (i.e., magnetic pressure less than plasma thermal pressure) and  $T_i < T_e$  are satisfied in the interval. Then we next examine the jump conditions in the magnetic field, plasma temperature, density, and solar wind velocity for the shock candidate events. We use the coplanarity theorem to calculate the shock normal in order to find the magnetic field normal component (magnetic flux) and velocity components (mass flux). The magnetic field geometry and the total pressure change across the shock are also checked. Finally, the slow shock is verified by the criteria:  $V_{sl} < V_n^* \leq V_{An}$ , where  $V_{SL}$  is the slow mode speed. The Alfvén velocity is  $V_A = B / \sqrt{4\pi Nm_p}$  and  $V_n^* = (\vec{V} - \vec{V}_s) \cdot \vec{n}$ , is the solar wind velocity  $\vec{V}$  relative to the shock velocity,  $\vec{V}_s$ , along the shock normal,  $\vec{n}$ , the latter which is obtained through coplanarity analyses. Defining the Alfvén velocity along the normal  $V_{An} = V_A \cos \theta_{Bn}$ , the Alfvén Mach number is  $M_A = V_n^* / V_{An}$ , where  $\theta_{Bn}$  is the angle between the magnetic field and shock normal.

## Results

Beyond 1 AU, in the ecliptic plane, the solar wind expands and stream-stream interactions become more pronounced. Large numbers of co-rotation interacting region (CIR) structures, fast forward, and fast reverse shocks have been detected. In these regions, high speed solar wind streams interact with low-speed streams, leading to a compression and pile-up of the plasma and magnetic field in front of the leading edges of the fast streams. Because of this interaction, hydromagnetic stresses propagate into both the slow and fast streams as large amplitude waves which ultimately steepen into a forward shock at the leading edge of a CIR and a reverse shock at the trailing edge. This effect becomes more significant with increasing heliocentric distances from the sun. If any, a slow-mode shock should occur at the boundary between a lower and a higher beta plasma region.

The pair of slow-mode shocks analyzed here are found in a compressed magnetic field region within a CIR. This region is bounded by both a fast forward shock-like discontinuity (f.f. discon.) and a reverse fast shock (r.f. shock) as marked in Figure 2. This CIR was encountered after Jupiter flyby when Ulysses was enroute to the southern

heliosphere (5.3 AU and 8.8°S heliographic latitude). Within the compressed magnetic field region, the magnetic field is much stronger ( $\sim 2.0$  nT) than in the non-compressed region ( $\sim 0.5$  nT). The solar wind velocity increases by  $\sim 100$  km/s, reaching  $\sim 500$  km/s. The plasma density significantly jumps from 0.2 to 1.8 cm<sup>-3</sup>; the proton temperature also jumps by approximately one order, to 10<sup>4</sup> K. Thus, the compressed region has a low value of  $\beta$  relative to the non-compression regions.

This pair of slow shocks actually occurred in the latter portion of the CIR, about one day before the reverse fast shock. We have expanded this period of data in Figure 3. The plasma properties are seen to be similar to those predicted by theory (Figure 1). The remarkable feature is the significant velocity jumps associated with both discontinuities (marked by vertical lines). At the first discontinuity (0710 UT on April 4, 1992) the velocity  $V_{sw}$  increases from 425 km/s to 463 km/s and the electron density ( $n_e$ ) is doubled (from 0.1 to 0.2 cm<sup>-3</sup>). The electron temperature does not show any obvious changes. Proton density ( $n_p$ ) increases from 0.6 to 1.2 cm<sup>-3</sup> while the proton temperature  $T_p$  jumps from 0.4 to 0.5x10<sup>5</sup>K. In contrast to these increases, the magnetic field decreases from 1.4 to 1.1 nT. After the decrease, the magnetic field has a gradual increase but then returns to the previous low level. The second interplanetary discontinuity occurred at 1105 UT. The magnetic field increases from 1.2 to 1.7 nT and  $V_{sw}$  increases from 447 km/s to 500 km/s.  $n_p$  decreases from 0.2 to 0.07 cm<sup>-3</sup> while  $T_p$  decreases from 1.5 to 0.6x10<sup>5</sup>K. On the basis of our slow shock criteria, both discontinuities are confirmed as slow-mode shocks. The first one is a forward shock, while the second one is a reverse shock.

All shock parameters are showed in Table 1. The forward slow shock has a normal in the direction of (-0.30, 0.32, 0.90) (mainly in the  $N$  direction) in a RTN coordinate system. The reverse shock's normal (0.34, -0.48, -0.81) is mainly along the negative  $N$  direction. These are generally opposite to the normal of fast mode shocks [Burton et al., 1996], because the normals generally point from the weak field to the strong magnetic field. Their downstream  $\theta_{Bn}$  is less than the upstream angle because of the weak downstream magnetic field. This is consistent with a slow shock's geometry. For both shocks, the upstream plasma velocity  $V_n$  is less than the normal Alfvén velocity  $V_{An}$ , but greater than the slow-mode velocity  $V_{sl}$ . However, the shocks are quite weak (lower Mach numbers) because the plasma velocity is very close to the  $V_{sl}$ . We also find that across the shocks the total pressure (magnetic plus thermal pressure) increases slightly. This is the main difference from a tangential discontinuity.

We have calculated the slow-mode shock speed using mass conservation:

$$V_s = \frac{N_2 \vec{V}_2 - N_1 \vec{V}_1}{N_2 - N_1} \cdot \vec{n} \quad (1)$$

Since the magnetic field is measured more accurately and more rapidly than the plasma density, we can also use the electric field conservation in the shock frame [Smith and Burton, 1988] to calculate the shock speed:

$$V_s = \frac{|\Delta \vec{V} \times \vec{B}_2|}{|\vec{B}_2 - \vec{B}_1|} \quad (2)$$

However, both methods yield nearly the same value for  $V_s$ . For the forward shock, the shock speed is about 60 km/s, while the reverse shock has a speed about 115 km/s. The speeds are similar to those for fast shocks. Burton et al. [1996] showed that fast shocks measured in Ulysses data between 4.0 and 5.0 AU have speeds ranging from 80 km/s to 180 km/s.

Using the shock speed, the shock thickness ( $\lambda_s$ ) may be estimated by measuring the magnetic field jump interval. For the forward shock, the jump interval is about 25 min, while for the reverse shock, it is ~20 min. After removing the spacecraft motion, we find shock thicknesses of  $7.5 \times 10^4$  km and  $12.6 \times 10^4$  km, respectively. This is equivalent to 65 and 144 ion inertial lengths ( $c/\omega_{pi} \sim 10^3$  km). This thickness is much larger than those of the slow shocks detected in the distant geomagnetic tail [Ho et al., 1995]. A theoretical study [Coroniti, 1971] suggests that slow shocks should have thicknesses of  $\sim 3-6 c/\omega_{pi}$ . One scenario explaining these large thickness is that the pair of shocks could have propagated some distance upstream after they were generated. The slow shocks become thicker because of solar wind velocity dispersion. Slow shocks will eventually disappear/dissipate as they propagate outward. They will be further weakened until their Mach number becomes close to unity, and then become a tangential discontinuity [Rosenau and Suess, 1977].

The slow shock dissipation mechanism is not well understood. It has been found that broadband plasma waves with frequencies ranging from ULF to VLF are detected in and near the shock layer in the distant geotail [Scarf et al., 1984]. The anomalous resistivity provided by the waves has been used to explain shock dissipation [Coroniti, 1971]. If such plasma waves are detected in interplanetary space associated with slow shocks, we can calculate the anomalous resistivity due to the waves and compare this with theoretical models. We have found that some wave bursts are detected by the Ulysses plasma wave instrument during the shock interval. Figure 4 shows the wave bursts measured from  $E_x$

antenna in three narrowband frequency channels (749, 857, and 1120 Hz) that occurred in the shock transition regions. These waves are similar to those observed at directional discontinuities and in magnetic holes [Lin et al., 1995] and near interplanetary shocks reported previously [Hess et al., 1998]. Considering the electron plasma frequency  $f_{pe} \sim 3$  kHz, proton plasma frequency  $f_{pi} \sim 67$  Hz, electron gyrofrequency  $f_{ce} \sim 44$  Hz, proton gyrofrequency  $f_{ci} \sim 0.025$  Hz, and the lower hybrid frequency  $f_{lh} \sim 1.1$  Hz, these wave bursts are likely to be ion acoustic waves which have been Doppler-shifted to the observed frequencies.

If indeed these ion acoustic waves provide anomalous resistivity to cause the shock damping, the magnetic Reynolds length ( $r_m$ ) should have the same order as the shock thickness  $\lambda_s$  [Coroniti, 1971], where

$$r_m = (c/\omega_{pi}) (v / \omega_{ce} M_A) \quad (3)$$

and the effective collision frequency (in cgs units) is:

$$\nu = E^2 \Delta f \omega_{pe} / 8\pi n k T_e \quad (4)$$

However, using all measured values, the calculation shows that  $r_m (=1/7500 c/\omega_{pi})$  is far less than the  $\lambda_s$  ( $\sim 50 c/\omega_{pi}$ ). Thus, this inconsistency suggests that the slow shock dissipation was not caused by an ion acoustic anomalous resistivity. The shock dissipation should be caused by some other mechanism(s). However, the upstream ion acoustic waves may suggest the existence of an ion forshock in front of the forward slow shock.

We have examined hourly average measurements of energetic particles from the HI-SCALE instrument [Lanzerotti, et al., 1992] during the period of the slow shock pair. Strong electron enhancements are detected in the two lowest energy channels (30-50 keV, and 50-90 keV). The enhancements are mainly seen in the direction of sectors 7 and 8 in telescope LEFS60, beginning about 07 UT and ending at 13 UT, as shown in Figure 5. The enhancements are less obvious in the two highest energy channels (90-165 keV, and 165-300 keV). LEFS60 has a  $60^\circ$  central view angle relative to the spin axis of the spacecraft. Around the spin axis, which is always pointed to the Earth, there are 8 directional sectors. The data are sampled in each sector every 12 s rotation period. Analysis shows that during this period, the magnetic fields are in the direction of sectors 7 and 8. Thus, these particles are propagating primarily along the background magnetic field. Since there are strong anisotropies in the pitch angle for these electrons (approximately 4 to 1 front to back anisotropy at the lowest energies). They are definitely accelerated by the slow shocks. Because both slow shocks are near quasi-parallel ( $\theta_{Bn} < 50^\circ$ ), magnetostatic reflection off the shock may be a significant acceleration mechanism [Tsurutani and Lin, 1985]. An initial

investigation shows that lower energy protons (50-73 keV) also show some enhancements around the slow shock. However, compared with the electrons, the enhancements in the energetic proton flux is smaller. A detailed analysis of the energetic electron acceleration by the slow shocks will be reported elsewhere.

### Summary

A pair of forward and reverse slow shocks is identified for the first time in the distant heliosphere using interplanetary magnetic field and plasma data from Ulysses. Both magnetic field discontinuities and jump conditions are found to satisfy all slow-mode shock criteria. The shock normal is mainly along the N direction. The downstream magnetic field  $\theta_{Bn}$  is less than the upstream  $\theta_{Bn}$ . The total pressure increases slightly across the shock from upstream to downstream. These properties are consistent with predictions for slow shocks. For both the forward and reverse shocks, the shock speeds are found to be 60 km/s and 115 km/s, respectively, similar to fast-mode shocks found in Ulysses measurements. Based on the shock ramp durations and the speeds, the calculated shock thickness is  $7.5 \sim 12.6 \times 10^4$  km, equivalent to  $65 \sim 144 c/\omega_{pi}$ . The thickness is much larger than those of slow shocks detected in the distant geotail and also larger than their inertial length as predicted by theory. This implies that the shocks have propagated some distance after their generation.

Low frequency wave bursts are found in the shock transition regions. These waves are probably ion acoustic waves. Calculations show that these waves cannot provide enough anomalous resistivity through wave-particle interactions for the shock dissipation. We also find strong electron enhancements in two low energy channels (30-50 keV, and 50-90 keV) around the shocks. Electron peaks begin about one hour before the forward shock and end about one hour after the reverse shock. The electrons are dominantly propagating along the background magnetic field. Because the slow shocks are near quasi-perpendicular shocks ( $\theta_{Bn} > 50^\circ$ ), magnetostatic reflection off the shock may be involved in the acceleration mechanism.

**Acknowledgments:** The research conducted at the Jet Propulsion Laboratory, California Institute of Technology was performed under contract to the National Aeronautics and Space Administration. The work done at the University of Minnesota was supported by NASA under contract NAS5-31219

## References

- Barnes, A., Collisionless damping of hydromagnetic waves, *Phys. Fluids*, **9**, 1483, 1966.
- Burton, M. E., et al., Ulysses out-of-ecliptic observations of interplanetary shocks, *Astronomy & Astrophysics*, **316**, 313, 1996.
- Burlaga, L.F., and J.K.Chao, Reverse and forward slow shocks in the solar wind, *J. Geophys. Res.*, **76**, 7516, 1971.
- Chao, J.K., and S. Olbert, Observation of slow shocks in interplanetary space, *J. Geophys. Res.*, **75**, 6394, 1970.
- Coroniti, F.V., Laminar wave-train structure of collisionless magnetic slow shocks, *Nuclear Fusion*, **11**, 261, 1971.
- Hess, R.A., R. J. MacDowall, B.Goldstein, M. Neugebauer, and R.J. Forsyth, Ion acoustic-like waves observed by Ulysses near interplanetary shock waves in the 3D heliosphere, *J. Geophys. Res.*, in press, 1998.
- Ho, C.M., B.T.Tsurutani, E.J.Smith and W.C.Feldman, A detailed examination of a X-line region in the distant tail: Observations of jet flows, Bz reversals and a pair of slow shocks, *Geophys. Res. Lett.*, **21**, 3031, 1994.
- Ho, C.M., B.T.Tsurutani, E.J.Smith, and W.C.Feldman, Properties of slow-mode shocks in the distant ( $> 200 R_e$ ) geomagnetic tail, *J. Geophys. Res.*, **101**, 15277, 1996.
- Kennel, C.F, J.P. Edmiston, and T. Hada, A quarter century of collisionless shock research, in *Collisionless Shocks in the Heliosphere: A Tutorial Review*, *Geophys. Monogr. Ser.*, **34**, 1, edited by R.G.Stone and B.T.Tsurutani, AGU, Washington D.C., 1985.
- Lanzerotti, L. J., et al., Heliospheric instrument for spectra, composition and anisotropy at low energies, *Astron. Astrophys. Suppl. Ser.* **92**, 349, 1992.
- Lin, N., P.J.Kellogg, R.J.MacDowall, A. Balogh, R.J. Forsyth, J.L. Phillips, A. Buttighoffer, and M. Pick, Observations of plasma waves in magnetic holes, *Geophys. Res. Letts.*, **22**, 3417, 1995.
- Petschek, H.E., Magnetic field annihilation, *AAS-NASA symposium on the physics of solar flares*, edited by W.N.Hess, NASA SP-50, P425, 1964.
- Pizzo, V.J., Interplanetary shocks on the large scale, in *Collisionless Shocks in the Heliosphere: A Tutorial Review*, *Geophys. Monogr. Ser.*, **34**, 51, edited by R.G.Stone and B.T.Tsurutani, AGU, Washington D.C., 1985.

- Richter, A.K., et al., Solar wind observations associated with a slow forward shock wave at 0.31 AU, Hundhausen, A.J., T.E.Holzer, and B.C.Low, Do slow shocks precede some coronal mass ejections?, *J. Geophys. Res.*, 90, 7581, 1985.
- Richter, A.K., Interplanetary slow shocks, Space and Solar Physics, 21, 23, *Physics of the Inner Heliosphere II*, Editors, R. Schwenn, E. Marsch, Springer-Verlag Berlin Heidelberg, 1991.
- Rosenau, P. and S.T. Suess, Slow shocks in interplanetary medium, *J. Geophys. Res.*, 82, 3643, 1977
- Scarf, F.L., F.V.Coroniti, C.F.Kennel, E.J.Smith, J.A.Slavin, B.T.Tsurutani, S.J.Bame, and W.C. Feldman, Plasma wave spectra near slow-mode shocks in distant magnetotail, *Geophys. Res. Lett.*, 11, 1050, 1984.
- Smith, E.J., and J.H.Wolfe, Observations of interaction region and corotating shocks between one and five AU: Pioneer 10 and 11, *Geophys. Res. Lett.*, 3, 137, 1976.
- Smith, E.J., and M.E. Burton, Shock analysis: Three useful new relations, *J. Geophys. Res.*, 93, 2730, 1988.
- Tsurutani, B.T., and R.P. Lin, Acceleration of > 47 keV ions and > 2keV electrons by interplanetary shocks at 1 AU, *J. Geophys. Res.*, 90, 1, 1985.

## Figure captions

Figure 1. A cartoon showing a pair of forward slow-mode shock (increases in the solar wind speed,  $V$ , plasma density,  $n$ , and temperature,  $T$ , vs. decrease in IMF  $B$ ) and reverse slow-mode shock (decreases in  $n$  and  $T$  accompanying a simultaneous increase in  $V$  and IMF  $B$ ). As a comparison, a pair of forward and reverse fast-mode shock also are shown.

Figure 2. Slow shock location relative to a compressed magnetic field region inside a CIR. This region lasts about seven days and is bounded by a fast forward shock type of discontinuity and a reverse fast shock. The pair of slow shocks (which interval is shaded) are in the rear portion of the CIR as marked.

Figure 3. A pair of slow-mode shocks identified. Across both shocks, solar wind velocity has a significant jump. Also ion temperature and density increase, while the magnetic field decrease. The plasma is in a low beta region with  $T_i < T_e$ .

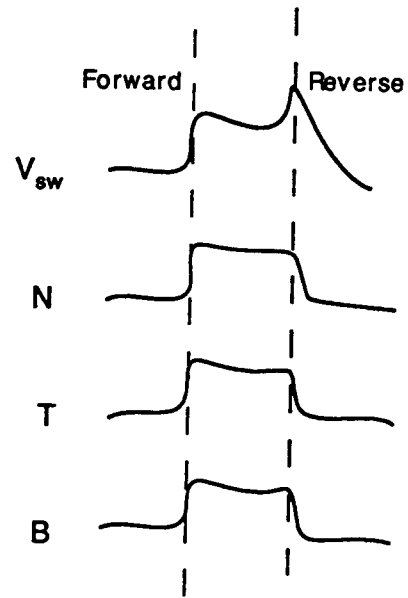
Figure 4. Plasma wave bursts associated with shocks. The waves appearing in three electric field narrowband channels are probably ion acoustic waves. Wave activity in the upstream around 0730 UT may suggest an existence of ion foreshock. Dotted lines show the total magnetic field.

Figure 5. HI-SCALE measurements for energetic electrons during the slow shocks. The data curve lines showed in the plots from top to the bottom are, respectively, from four channels: E1 (30-50 keV), E2 (50-90 keV), E3 (90-165 keV) and E4 (165-300 keV). In the directional sectors 7 (left) and 8 (right), there are significant electron enhancements in two low energy channels (30-50 keV, and 50-90 keV) around the shocks.

Table 1. Slow-mode Shock Parameters for the Event of April 4, 1992

Shock Parameters	Forward Shock 0710UT	Reverse shock 1105UT
$n$ in RTN	-0.30, 0.32, 0.90	0.34, -0.48, -0.81
$B_1$ , nT	1.44	1.71
$B_2$ , nT	1.14	1.18
$B_n$ , nT	1.12	1.16
$\theta_{Bn1}$	39°	47°
$\theta_{Bn2}$	10°	10°
$V_1$ , km/s	424	499
$V_2$ , km/s	465	447
$N_{p1}$ , cm <sup>-3</sup>	0.04	0.07
$N_{p2}$ , cm <sup>-3</sup>	0.10	0.20
$T_{p1}$ , x10 <sup>5</sup> K	0.50	0.59
$T_{p2}$ , x10 <sup>5</sup> K	1.10	1.45
$V_s$ , km/s	60	115
$V_{An}$ , km/s	92	87
$V_n^*$ , km/s	29	44
$V_{sl}$ , km/s	26	20
$M_A$	0.31	0.50
$\Delta P_{tot}$ , dyn/cm <sup>2</sup>	0.05x10 <sup>-10</sup>	0.01x10 <sup>-10</sup>

a) Fast-mode Shock



b) Slow-mode Shock

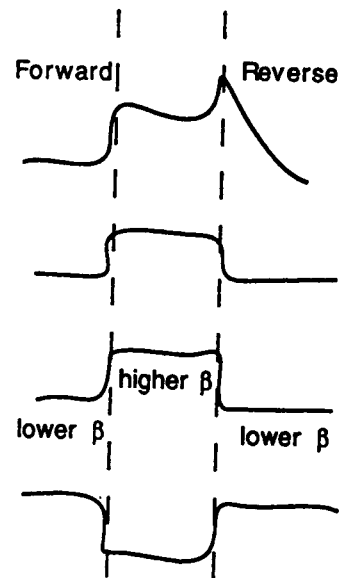


Figure 1

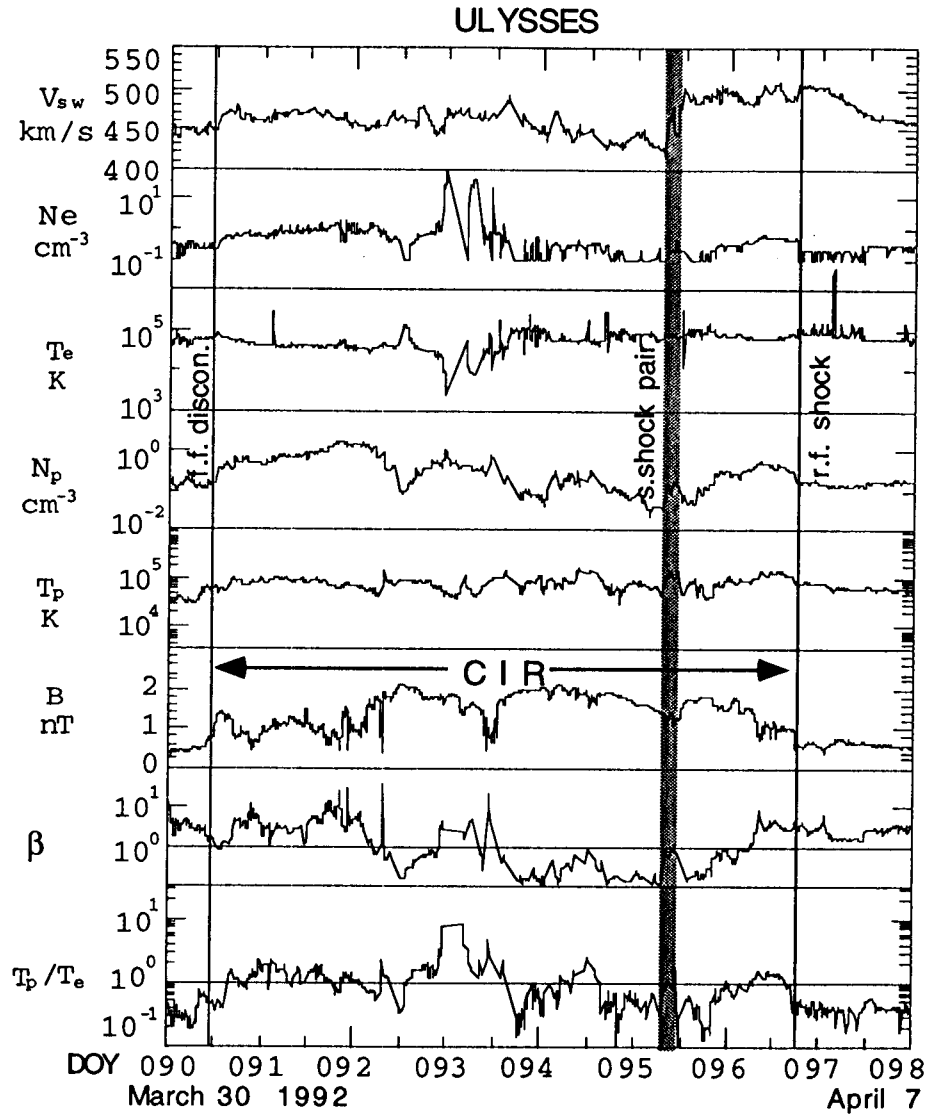


Figure 2

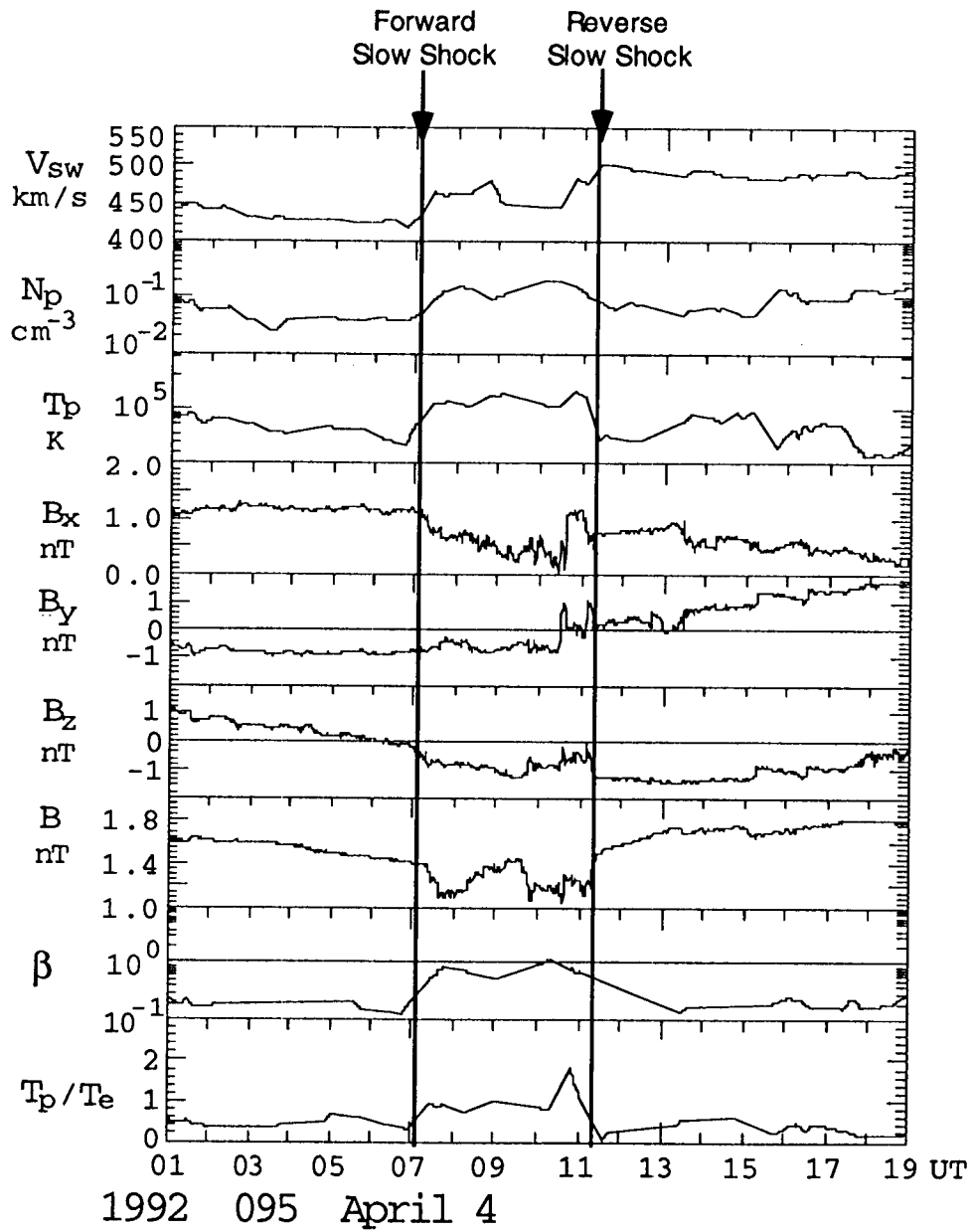


Figure 3

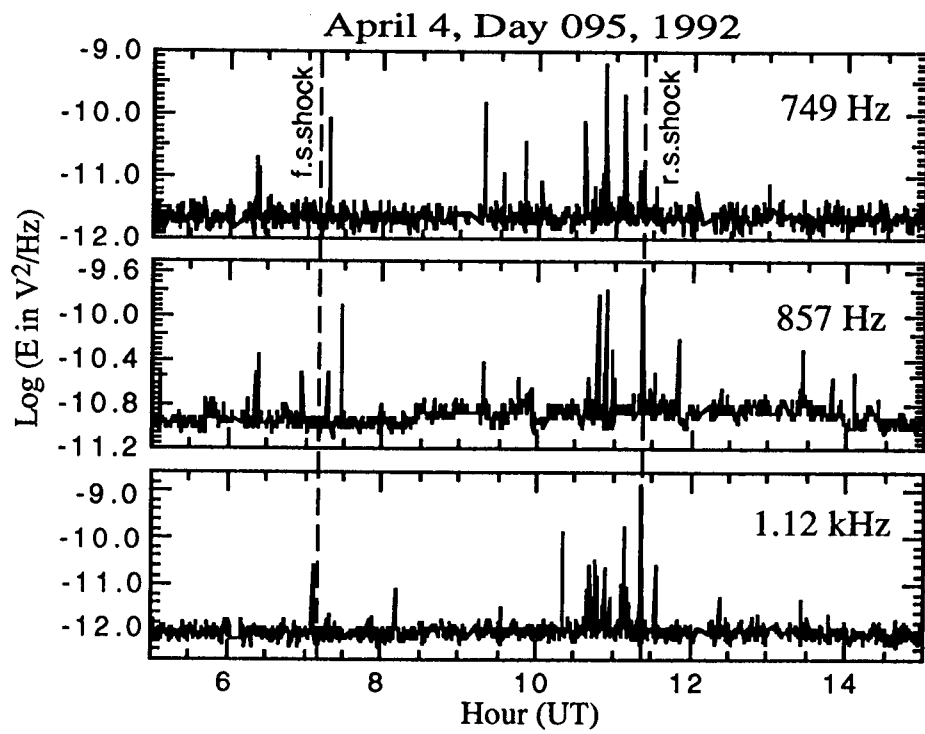


Figure 4

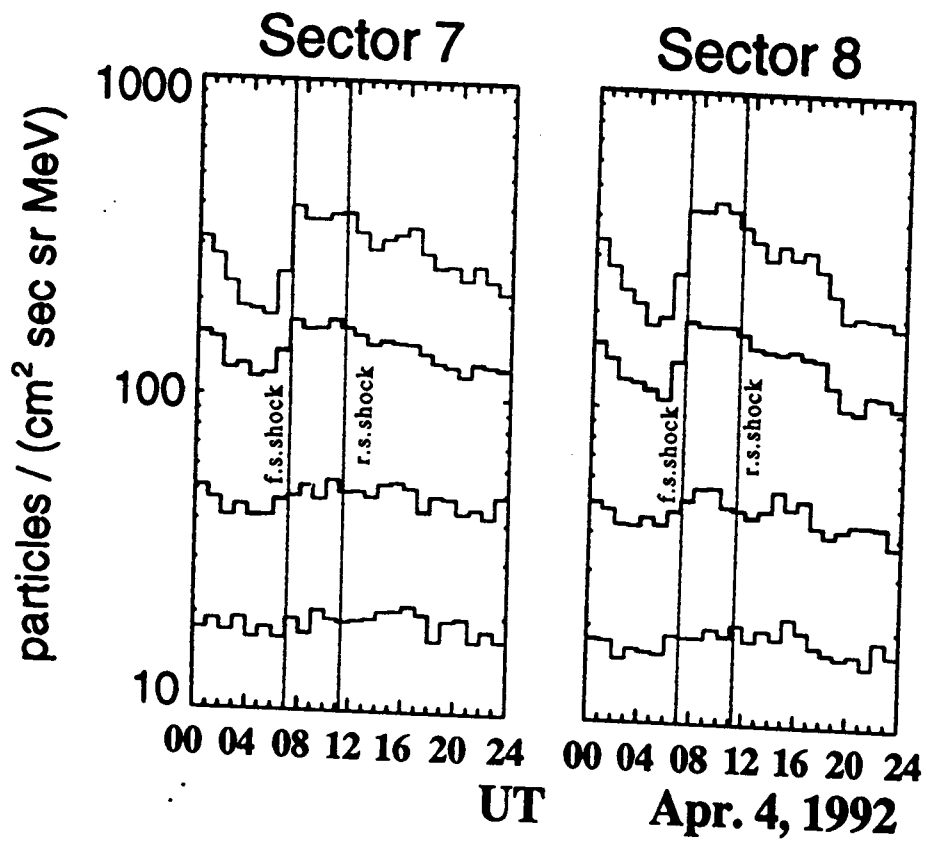


Figure 5